

# **Compressed Sensing: Single Pixel Imaging in Short-Wave Infrared Spectrum**

**Examensarbete**

TQET33

Andreas Brorsson, Andbr981, (911023-1215)

Linköping, 2017

# 1 Introduction

The development and research of compressed sensing applied to a single pixel camera (SPC) is a relative new area in signal processing with the first functioning camera architecture in 2006. Since then numerous improvements and methods have been proposed how to capture images. In this section a introduction to the SPC architecture and a brief introduction of compressed imaging is presented followed by the aim, research questions and thesis outline.

## 1.1 Background

Compressed sensing (CS) allows reconstruction of a sparse signal being sampled with far fewer samples required to fulfill the sampling theorem. Swedish Defence Research Agency (FOI) became interested in the subject some years ago and tests potential applications. One of the potential applications are a camera with a single pixel which can reconstruct a scene, therefore FOI built a SPC platform in the short-wave infrared (SWIR) spectrum for the purpose to study and evaluate this kind of system.

The SWIR spectrum is electromagnetic radiation with wavelengths between 700 - 2500 nm and SWIR cameras can therefore capture images illuminated by the sun, moon, star light and airglow thus works both by day and night. SWIR light can to some extent pass through smoke and fog which makes it robust camera for day and night applications. Some camouflage that is hard to spot in visual spectrum is visible in the SWIR spectrum. The system used in this master's thesis uses a digital micromirror array (DMD) to sample the light from the scene. The system will sample less single pixel measurements than the number of pixels in the reconstructed image with the drawback that it has to capture each measurement in consecutive order instead of all at the same time.

## 1.2 Compressive sensing & imaging

Compressive sensing is a new sampling strategy which reconstructs a compressible or sparse signal by finding solution to undetermined linear system where the number of measurements  $M$  is less than the number of data points  $N$  in signal. Two constraints need to be fulfilled to apply compressed sensing sampling: the sampled signal needs to be spares in some basis e.g. Fourier or gradient, the second condition is that the measurement matrix must be incoherent with the sparse transform. The characteristic undetermined linear system in CS is defined as  $\mathbf{y} = \Phi\mathbf{x}$  where  $\mathbf{y}$  contains the measurements from the measurement matrix  $\Phi$  sensing the signal  $\mathbf{x}$ . In figure 1 such linear equation system is shown.

$$\begin{matrix} \mathbf{y} \\ \begin{matrix} y_1 \\ y_2 \\ y_3 \\ \vdots \\ y_M \end{matrix} \end{matrix} = \boxed{\Phi} \quad \begin{matrix} \mathbf{x} \\ \begin{matrix} x_1 \\ x_2 \\ x_3 \\ x_4 \\ \vdots \\ x_N \end{matrix} \end{matrix}$$

The diagram illustrates the linear equation system  $\mathbf{y} = \Phi\mathbf{x}$ . On the left, the vector  $\mathbf{y}$  is shown as a column of measurements  $y_1, y_2, y_3, \dots, y_M$ . An equals sign follows. To the right of the equals sign is a large rectangular box labeled  $\Phi$ , representing the measurement matrix. This matrix is filled with entries  $\Phi_1, \Phi_2, \Phi_3, \dots, \Phi_M$ , corresponding to the measurements  $y_1, y_2, y_3, \dots, y_M$  respectively. To the right of the matrix  $\Phi$  is another column vector labeled  $\mathbf{x}$ , representing the signal, with entries  $x_1, x_2, x_3, x_4, \dots, x_N$ .

Figure 1: CS undetermined linear system

Scientists at Rice university in Texas, USA realized that the new method could be used to create a new camera architecture with a single photo diode in the sensor, the single pixel camera was born and thus a new sub field of compressed sensing was created called compressive imaging.

To be able to apply CS to imaging in the first place the constraints in CS needs to hold for images as well. The first requirement is that the signal needs to be compressible or sparse in some basis which natural images is known to be because they can be compressed using for example JPEG (Descrete cosine transform), JPEG2000 (Wavelet). The second constraint is that the measurement matrix must be incoherent with the sparse transform which for example white noise or some structure with the same property as white noise.

### 1.3 System architecture

The SPC in this master's thesis was designed with reflecting telescope optics to act as a lens to focus the scene. As seen in figure 2 light from the scene enters through the aperture in the camera where the primary mirror focus the light the via the secondary mirror onto the DMD. To this point, the SPC works like a conventional camera with a DMD where the image sensor would be placed in the convectional camera. The SPC has an digital micromirror array in the focal point which resemble an image sensor but instead of photo diodes for each pixel there is a tiny mirror which individually can ether reflect light 12 degrees to the right or left as seen in figure 2. The incomming focused light can ether be dumped or it can be reflected into the single pixel SWIR detector through an lens. SWIR is the short wave infrared spectrum and is defined in the wavelengths between 700 to 2500 nm just where humans perception of red wavelength ends SWIR starts.

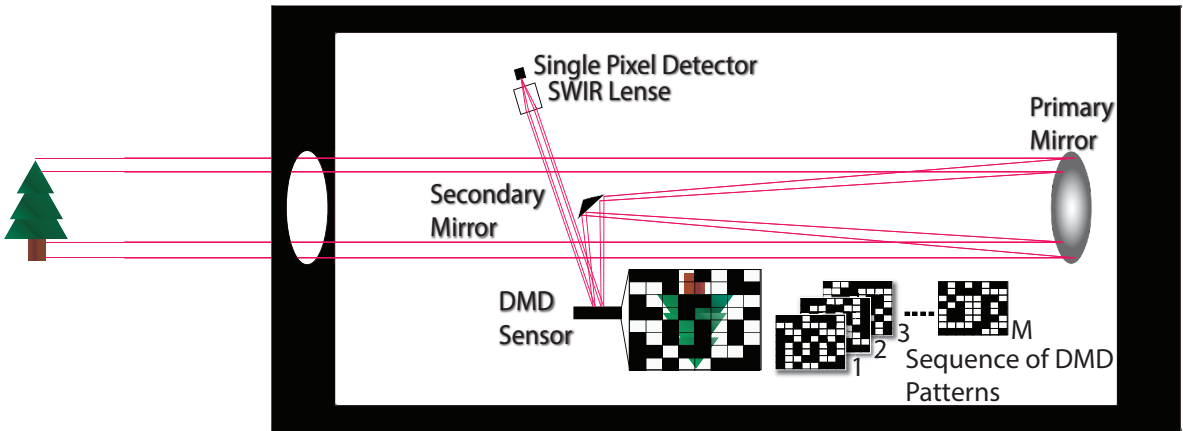


Figure 2: System overview

To connect the architecture with the math from CS it can be interpreted as, the light from the scene which is focused on the DMD is the desired signal  $\mathbf{x}$ , the image. The DMD can individually set each mirror the ether direct the light from each 'pixel' to the single pixel sensor or dump the light i.e a spatial light modulator (SLM). The DMD sets a pattern of pixel of intress which is a measurement matrix  $\Phi_m$  to be summarized in the single pixel sensor  $y_m$  as a measurement. One measurement is the inner product of a measurement matrix and the signal,  $\Phi_m \times x = y_m$ . To complete a full measurement the process is repeated with different measurement matrices set on the DMD to the full undetermined linear system  $\mathbf{y} = \Phi\mathbf{x}$ .

### 1.4 Measurement matrix & reconstruction

How is the measurement matrix chosen? As told before the measurement matrix needs to be incoherent with the sparse transform and the DMD can only direct he light or not which mathematically is ether a zero or a one. The research tells that for example a i.i.d. Gaussian distribution with equal probability of a zero or one will with high probability be incoherent with a natural image scene. But how about the first constraint that the signal  $\mathbf{x}$  needs to be sparse or

compressible in some basis? Often natural images is not sparse in the spatial domain unless the scene is for example the night sky, well a good property of CS that the scene can be transformed to another basis like this,

$$\mathbf{y} = \Phi \mathbf{x} \Leftrightarrow \mathbf{y} = \Phi \Psi \Theta, \quad (1)$$

where  $\Psi$  is a sparsifying basis for example to the DCT or Wavelet basis. And  $\Theta$  is the coefficients vector which is more sparse than the spatial coefficient vector  $\mathbf{x}$ . And the transformation will not compromise the incoherence between the reconstruction matrix  $A = \Psi \Phi$  and the coefficients  $\Theta$  in the new basis. This means that the signal  $\mathbf{x}$  will be reconstructed with optimization in a more sparse basis  $\Theta$  and then transformed back to the spatial domain.

What is special about CS is not just how the problem is presented but also how to solve it. It is known that an undetermined linear system has infinite many solutions so how does the signal get recovered? CS exploits the characteristics of the signal  $x$  which is known to be sparse in some basis. With for example  $\ell_1$  optimization,

$$\hat{\Theta} = \arg \min \|\Theta\|_{\ell_1} \text{ subject to } \Phi \Psi \Theta = y, \quad (2)$$

which means that  $\ell_1$  optimization minimizes the non-zero elements of  $\Theta$  and can exactly reconstruct a K-sparse vector or approximate a compressible vector. The exact recovery can be accomplished with high probability using  $M \geq \mathcal{O}(K \log(N/K))$  measurements. This is why CS is powerful, it enables sub-Nyquist measurements with exact recovery in the noiseless case which can be approximated in real applications.

In the compressed imaging case where noise is present an other optimization algorithm has shown to be more successful at recovering images: total variation. Total variation regularization minimizes the magnitude of the gradient in the image and doing so it preserves edges and piece-wise constant structure in the image which is desired.

## 1.5 Motivation

Why would a SPC be beneficial to a conventional camera? The SPC has more components and several measurements have to be made over time while a regular camera measures all pixels on the sensor at the same time, and the reconstruction shifts the burden to the processor. There are two major reasons why a SPC is of interest, it is not to compete with the conventional cameras in the visual spectrum where cameras in all price ranges and quality already exist and are relatively cheap to build. The focus lies in more exotic spectrum of light like SWIR or Terahertz (X-ray) wavelengths where the image sensors are hard to build which brings up cost and the ability to create high resolution sensors. With CS and the SPC architecture manufacturing cost can be significantly reduced while the image resolution increases. For an example a state of the art SWIR camera cost about half a million SEK which can be reduced by a factor of 100 with a SPC with the same resolution.

## 1.6 Aim

What image quality can be achieved in natural images captured with a single pixel camera in daylight using state of the art methods?

## 1.7 Research questions

- How can the quality of images reconstructed by CS or a SPC be evaluated?
- What is the state of the art method to capture and reconstruct images using a SPC architecture?
- What image quality is achieved using state of the art methods applied to the SPC?

## **1.8 Limitations**

- The hardware rig provided by FOI
- 

## **1.9 Thesis outline**

## 2 Related work

In this section important, relevant and fundamental articles to this master's thesis is presented each with a summary. The articles covers compressed sensing theory applied to compressed imaging, SPC architecture and how to evaluate the images i.e. the fundamental source of information on how to build a state of the art SPC system and how to evaluate its performance.

### 2.1 Compressive sensing

### 2.2 Compressive imaging

- In [1] David L. Donoho proposed the framework of compressed sensing and its application to images.
- 
- [2] Fast and Efficient Compressive Sensing Using Structurally Random Matrices. Describes that SRM works and why.

### 2.3 Evaluation

- Al Boviks book the essential guide to image processing [3] contains the majority of fundamental image processing techniques and measurements. Two image quality metrics of interest is PSNR and SSIM which can be used when a reference image is available.
- [4] A Feature-Enriched Completely Blind Image Quality Evaluator describes how the no reference image quality assessment tool IL-NIQE works and compares to other NR-IQA algorithms. In the article a comparison with other state of the art NR-IQA is conducted which concludes that IL-NIQE is the best over all NR-IQA tool. This kind of QA is useful when there is no reference image available, which is true when taking photos with the SPC.

### 2.4 Analysis

### 3 Method

New method introduction depending on how the disposition will be in the final form

In order to answer the research questions stated in section 1.7 a state of the art SPC, experiments and evaluation methods needs to be set up. In this section the SPC hardware and image sensing and reconstruction scheme is described.

#### 3.1 Single pixel camera architecture & hardware

FOI designed the SWIR SPC platform using a DMD, a Newtonian telescope and a single pixel SWIR detector. The system also has a reference camera in the visual spectrum which can capture images if all micro mirrors in the DMD are turned away from the single pixel sensor and towards the reference camera, it can also be used to check that the patterns are displayed correct on the DMD.

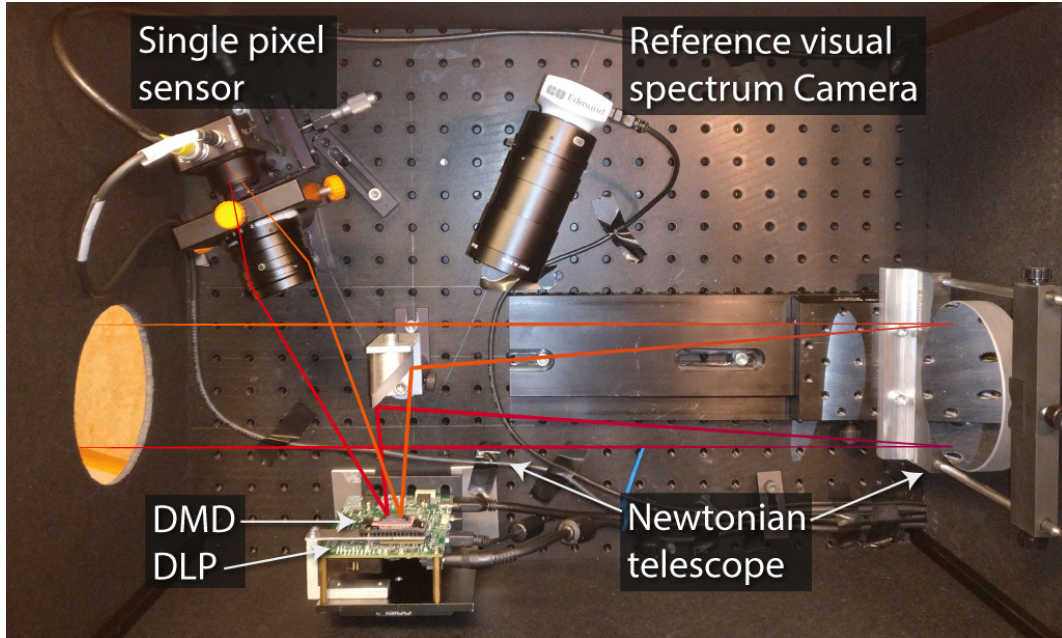


Figure 3: Single pixel imaging system (SPIS), adopted from [5].

As seen in figure 3 light from the scene is focused by the Newtonian telescope and reflected onto the DMD. The mirrors on the DMD can turned individually either into the single pixel sensor or the reference camera. The DMD acts as a Spatial Light Modulator (SLM) and reflects different patterns which is 'summed up' in the single pixel sensor as an intensity. The reconstructed image from the system will have the same resolution as the DMD patterns. The DLP is the DMD control unit which controls which patterns are displayed on the DMD either by reading images from memory or the video port.

##### 3.1.1 Newtonian telescope

A Newtonian telescope is a reflecting telescope, using a concave primary mirror and a flat diagonal secondary mirror, see figure 3. In this set-up the telescope act as a lens focusing the scene onto the DMD. The motivation to use a Newtonian telescope instead of a lens system is partly that chromatic aberration is eliminated and partly that a reflective optical system works over a greater range of wavelengths that includes SWIR, near infrared (NIR) and the visible spectrum.

### 3.1.2 DLP and DMD

The DMD (Texas Instruments DLP4500NIR) is a matrix of micro mirrors that can be individually tilted  $\pm 12^\circ$  and reflects wavelengths in the range 700-2500 nm. The DMD is controlled by the DLP (DLP LightCrafter 4500) which can be controlled either by video port (HDMI) or by the internal flash memory. The internal memory can theoretically be faster than the video port but due to constraints in both memory and memory bandwidth the fastest measurement matrix rate gets stuck at 270 – 300 Hz. The video port can be operated at 120 Hz and display one bit plane at the time from a 24 bit signal, which gives a maximum measurement matrix rate at  $120 \times 24 = 2880$  Hz, but in the current configuration only 60 Hz frame rate was achieved giving a measurement matrix rate at 1440 Hz. At this rate with the number of measurements relative to number of pixels in reconstructed image between 20% – 30% a  $256 \times 256$  pixel images data would be acquired in 9 – 13 seconds and for a  $512 \times 512$  pixel image 36 – 53 seconds. To control the DMD the software 'DLP LightCrafter 4500 Control Software' is used.

The DMD in the setup is constructed with a diamond shaped pattern instead of a regular square grid which is used in regular camera image sensors. The diamond shape causes the index of each mirror to be skewed against what a normal grid would look like. As seen in figure 4 the indexes of the mirrors column is two mirror column arrays wide while a row is a single row.

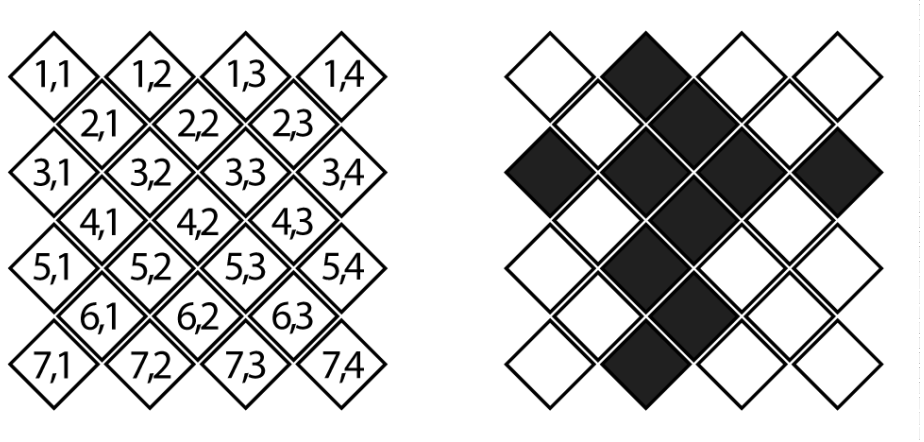


Figure 4: DMD matrix, left shows each tiles index and right shows second row and second column in black.

Because the reconstruction algorithm and measurement matrix needs to be a square matrix with the side length with a power of 2 the resulting images ratio would be 2 to 1 while the image should have the ratio 1 to 1. The resulting image would need to be transformed into the real ratio where information potentially gets lost. Therefore the index of mirrors was changed so that each 'pixel' gets two mirrors as seen in figure 5. This will result in rows and columns gets equal amount of space and the aspect ratio will be preserved to 1 to 1.

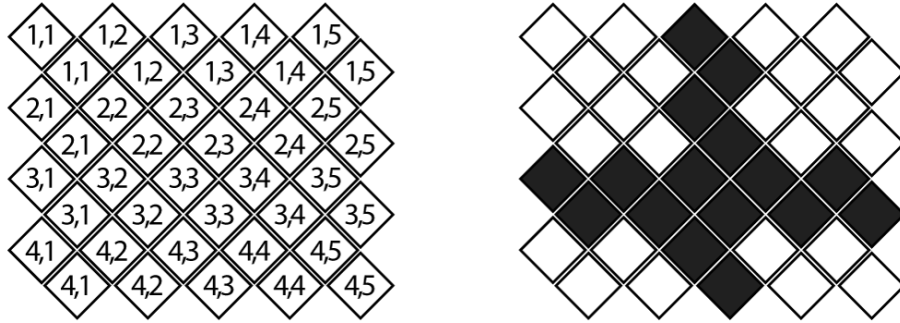


Figure 5: DMD matrix, left shows each tiles index and right shows third row and third column in black.

Connect the DMD to CS and the physical aspect (every mirror is an pixel)

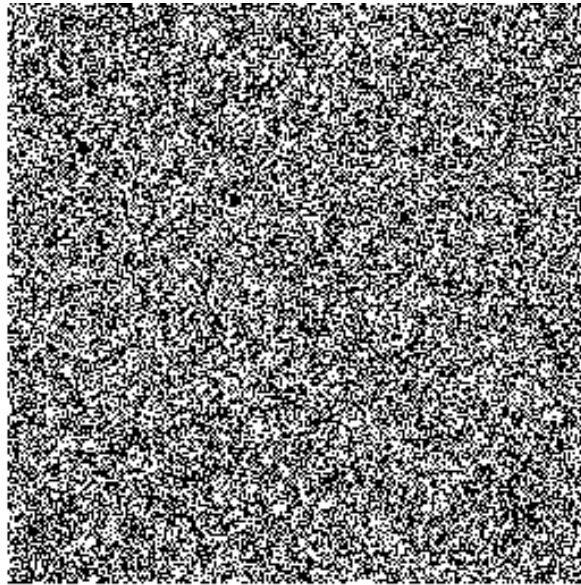


Figure 6: A typical measurement matrix presented on the DMD with the resolution  $256 \times 256$  pixels.

### 3.1.3 Lens

The lens mounted on the single pixel sensor is an 50mm SWIR Fixed Focal Length Lens with an variable appature from f1.4 designed for wavelengths raging from the 800 nm in the visual spectrum to 2000 nm in the SWIR spectrum. [6]

### 3.1.4 Single pixel sensor

The single pixel sensor is a Thorlabs PDA20C/M and is sensitive in wavelength range 800-1700 nm which is beyond the visual spectrum (390-700 nm). The sensor outputs an analog signal in volt which the sampler converts to a discret value. [7]

### 3.1.5 Signal spectrum

All components characteristics assembled the wavelengths that pass through the system and measured in the single pixel sensor is between 800-1700 nm.

## 3.2 Compressive imaging

Write introduction to CS, create some intuition

The single pixel sensor captures a scene by measuring the light intensity focused into the detector reflected from the DMD matrix. The DMD sensing matrix changes to obtain new measurements,  $M$  unique sensing matrix measurements is captured to reconstruct an image with  $N$  pixels. Each sensing matrix index is encoded either by a one or a zero (turning the mirror onto or away from the sensor). The compressive imaging sampling model is defined as

$$\mathbf{y} = \Phi \mathbf{x} + \epsilon, \quad (3)$$

where,  $\mathbf{x}_{N \times 1}$  is the signal (image) with  $N$  samples (pixels),  $\mathbf{y}_{M \times 1}$  is the vector with  $M$  measurements,  $\Phi_{M \times N}$  is the measurements matrix (each unique sensing matrix  $\Phi_{1 \times N}$  as a row vector) and  $\epsilon$  is the noise. In conventional sampling the number of measurements  $M$  needs to be at least equal to the number of samples  $N$  to recover the signal but CS states that  $M$  can be relatively small compared to  $N$  given how compressible the signal is. The signal  $\mathbf{x}$  can be represented as

$$\Psi \Theta = \mathbf{x}, \quad (4)$$

where,  $\Psi_{N \times N}$  is some basis matrix and  $\Theta_{N \times 1}$  is the coefficients where  $\theta$  is  $K$ -sparse.  $K$ -sparse means that the signal  $\mathbf{x}$  has  $K$  non zero elements in basis  $\Psi$ ,  $\|\Theta\|_0 = K$ . Given equation 4, equation 3 can be expand to

$$\mathbf{y} = \Phi \mathbf{x} + \epsilon = \Phi \Psi \Theta + \epsilon = \mathbf{A} \Theta + \epsilon, \quad (5)$$

where,  $\mathbf{A}_{M \times N} = \Phi \Psi$  is the reconstruction matrix. The last statement is what makes CS powerful, a signal which is not sparse can be sampled with measurement matrix  $\Phi$  and then reconstructed with reconstruction matrix  $\mathbf{A}$  in a basis where  $\mathbf{x}$  is sparse or compressible.

## 3.3 Measurement matrix & Restricted isometry property (RIP)

Introduce the topic.

In the noiseless case exact recovery of the image  $\mathbf{x}$  is achievable if RIP holds for the reconstruction matrix  $\Phi \Rightarrow \Phi \Psi = \mathbf{A}$ , the constraint is defined as,

$$(1 - \delta_K) \|\mathbf{x}\|_{\ell_2}^2 \leq \|\mathbf{Ax}\|_{\ell_2}^2 \leq (1 + \delta_K) \|\mathbf{x}\|_{\ell_2}^2, \quad (6)$$

where  $\delta_K \in [0, 1]$  is the smallest constant to satisfy RIP for a  $K$ -sparse signal  $\mathbf{x}$ . To determine a sampling matrix is a NP-hard problem (which means that there are no feasible way of creating a optimal reconstruction matrix) and generally  $\mathbf{x}$  is not known and varies which means that there are no general optimal reconstruction matrices for natural images. The solution is to find a general reconstruction matrix that satisfies RIP with high probability. The solution which also should be incoherent with the base matrix  $\Psi$  is to construct the measurement matrix using a i.i.d random distribution which gives  $\delta_K \ll 1$  with high probability. Using random measurement matrices the number of measurements needed to satisfy RIP with high probability is  $M \geq O(K \log(N/K)) \ll N$ .

The problem using random matrices is that they need to be stored in memory for the reconstruction algorithm, when the image resolution is increased the measurement matrix increases exponentially. For images with resolution of  $512 \times 512$  and larger the data gets infeasible for a normal computer to handle. Fortunately using fast transforms in the reconstruction algorithm can exclude using vector multiplication resulting in faster reconstruction and the need to store the measurement matrix in memory. But in order to do so special measurement matrices are used, in this master's thesis the sequency ordered Walsh Hadamard measurement matrix will be used with the TVAL3 reconstruction algorithm described in section 3.4.1.

### 3.3.1 Sequency ordered Walsh Hadamard measurement matrix

Besides from eliminating the need to store the measuring matrix for reconstruction the sequency ordered Walsh Hadamard (SOWH) matrix can be generated when sent to the DMD eliminating the need to store the matrix at all. SOWH has the same characteristics and properties of an i.i.d random matrix and therefore also fulfills the RIP condition with high probability and research has shown that there is no significant loss in recovery of the signal relative i.i.d random measurement matrix. An other property of SOHW is that it only contains -1 and 1 which easily be converted to 0 and 1 when sent to the DMD.

find the source ref

The naturally ordered Hadamard matrix of dimension  $2^k$ ,  $k \in \mathbb{N}$  are constructed by the recursive formula

$$H_0 = 1, \quad (7)$$

$$H_1 = \begin{bmatrix} 1 & 1 \\ 1 & -1 \end{bmatrix}, \quad (8)$$

and in general,

$$H_k = \begin{bmatrix} H_{k-1} & H_{k-1} \\ H_{k-1} & -H_{k-1} \end{bmatrix} = H_1 \oplus H_{k-1} \quad (9)$$

where  $\oplus$  denotes the Kronecker product. To construct the sequency ordered Walsh Hadamard matrix from the naturally ordered Hadamard matrix three steps is required:

- Convert row index to binary.
- Convert the binary row index to gray code.
- Apply bit reverse on the gray code index.

then order the rows after the bit reverse to obtain the sequency ordered Walsh Hadamard matrix.

$n_H$	0	1	2	3
Binary	00	01	10	11
Gray code	00	01	11	10
Bit-reverse	00	10	11	01
$n_W$	0	2	3	1

Table 1: How to convert a naturally ordered Hadamard matrix to a sequency ordered Walsh Hadamard matrix by shifting row with index  $n_W$  to  $n_H$

for example

$$H_2 = \begin{bmatrix} 1 & 1 & 1 & 1 \\ 1 & -1 & 1 & -1 \\ 1 & 1 & -1 & -1 \\ 1 & -1 & -1 & 1 \end{bmatrix} \Rightarrow W_2 = \begin{bmatrix} 1 & 1 & 1 & 1 \\ 1 & 1 & -1 & -1 \\ 1 & -1 & -1 & 1 \\ 1 & -1 & 1 & -1 \end{bmatrix}. \quad (10)$$

To use the sequency ordered Walsh Hadamard matrix as an measurement matrix the fist row is omitted, permutations to the columns is performed,  $M$  rows are choosen at random and the indices with a  $-1$  is shifted to 0. This last step is required to convert the measurement matrix so it gets the characteristics of an i.i.d random matrix and thus fulfill the RIP condition. How the matrix was permuted is stored because the reconstruction algorithm uses that information. [8], [9].

### 3.4 Reconstruction method

To reconstruct the image  $\mathbf{x}$  the sparsest set of coefficients in  $\Theta$  is desired. The optimal approach to find these coefficients would be to use  $\ell_0$  minimization

$$\hat{\theta} = \arg \min \|\theta\|_0 \text{ subject to } \mathbf{y} = \mathbf{A}\theta. \quad (11)$$

Simply minimizing nonzero indices  $\Theta$  in the sparsifying basis  $\Psi$ , but this problem is known to be NP-hard. A better approach is the  $\ell_1$  minimization, for example Basis Pursuit denoise (BPDN),

$$\hat{\theta} = \arg \min \|\theta\|_1 \text{ subject to } \|\mathbf{y} - \mathbf{A}\theta\|_2 < \epsilon. \quad (12)$$

In 2006 Donoho [1] for the fist time guarantied theoretical  $\ell_0/\ell_1$  equivalence which holds in the CS case, which means using a  $\ell_1$  minimizer is guaranteed to find the sparsest solution in polynomial time in the noiseless case which can be approximated in the noisy and compressible signal case. The drawback with the  $\ell_1$  minimizer is that it require more measurements than the optimal case with  $\ell_0$  but it is still  $M \ll N$ . Since 2006 many more types of optimization algorithms has evolved which solves the problem with different methods but with the same goal: finding the largest most significant coefficients of  $\theta$ .

#### 3.4.1 Total variation

##### A closer look at the TVAL3 algorithm

The reconstruction algorithm that was chosen in this Master's thesis was a total variation regularization algorithm. Natural images often contains sharp edges and piecewise smooth areas which the TV regularization algorithm is good at preserving.

TV AL Augmented Lagrangian -

Augmented Lagrangian methods are a certain class of algorithms for solving constrained optimization problems. They have similarities to penalty methods in that they replace a constrained optimization problem by a series of unconstrained problems and add a penalty term to the objective; the difference is that the augmented Lagrangian method adds yet another term, designed to mimic a Lagrange multiplier.

AL Alternating Direction -

Why use the  
TV algo-  
rithm

Alternating direction methods are a common tool for general mathematical programming and optimization. These methods have become particularly important in the field of variational image processing, which frequently requires the minimization of non-differentiable objectives. This paper considers accelerated (i.e., fast) variants of two common alternating direction methods: the Alternating Direction Method of Multipliers (ADMM) and the Alternating Minimization Algorithm (AMA). The proposed acceleration is of the form first proposed by Nesterov for gradient descent methods. In the case that the objective function is strongly convex, global convergence bounds are provided for both classical and accelerated variants of the methods. Numerical examples are presented to demonstrate the superior performance of the fast methods for a wide variety of problems.

The alternating direction method of multipliers (ADMM) is an algorithm that solves convex optimization problems by breaking them into smaller pieces, each of which are then easier to handle. It has recently found wide application in a number of areas. On this page, we provide a few links to interesting applications and implementations of the method, along with a few primary references.

ADMM is used in a large number of papers at this point, so it is impossible to be comprehensive here. We only intend to highlight a few representative examples in different areas. To keep the listing light, we have only listed more detailed bibliographic information for papers that are not easy to find online; in any case, the information given should be more than enough to track down the papers.

AL Algorithm

### 3.5 Image capturing and processing chain

A section describing the process from sampling the signal to complete image. Which algorithms was used and an introduction to how the signal looks at different stages of the process.

Flowchart of the whole process.

- A video containing the measurement matrix with 24 matrices per frame was streamed was stream through a HDMI port with the software MPC-HC. The DLP shows one bit plane at the time on the DMD until next frame arrives.
- MATLAB was used for signal processing.
- Acquire signal: Start sampling signal from the single pixel sensor, and start chain of measurement matrices.
- From the raw signal: Extract value from each measurement matrix, Signal processing compensating for illumination change and delete if necessary disruption. We use the knowledge that the signal should be stationary.
- Reconstruct image from signal.
- Image processing: median filter.

### 3.6 Evaluation: Image quality assessment

The evaluation will be divided in to two categories: reconstructed images from synthetic data and images reconstructed from data acquired by the SPC.

The evaluation on synthetic data is focused on evaluating the performance of the measurement matrix and reconstruction algorithm. Evaluating synthetic data gives two possibilities that can not be achieved with images reconstructed using the SPC which is that there is a reference image which the resulting image can be compared to.

Reconstructed image from synthetic data is acquired by creating a signal  $\mathbf{y}_{M \times 1}$  taking the inner product of  $\mathbf{y} = \Phi\mathbf{x} + \epsilon$  where,  $\mathbf{x}$  is the synthetic image reshaped to a vector,  $\Phi$  is the measurement matrix with the desired amount of measurements  $M$  and synthetic noise  $\epsilon$  which can be regulated to simulate different conditions, then using the reconstruction algorithm on the signal  $\mathbf{y}$  to obtain the reconstructed image  $\hat{\mathbf{x}}$ . Because the measurement matrix and reconstruction algorithm is independent of the SPC hardware the subsystem can be evaluated independently. Two advantages of evaluation the sensing and reconstruction independently of the SPC is that parameters such as number of measurements and noise can be regulated easy and the second advantage is that a reference image is available for comparison.

With a reference image available two image quality assessments are performed on the result from the simulation: Peak signal-to-nise ratio (PSNR) and SSIM. PSNR is defined as

$$\text{PSNR}[f(x, y), g(x, y)] = 10 \log_{10} \frac{E^2}{\text{MSE}[f(x, y), g(x, y)]} \quad (13)$$

where,  $f(x, y)$  and  $g(x, y)$  is intensity in pixel  $(x, y)...$

### 3.7 Method criticism

- No Reference Image Quality Assessment is not designed for SWIR images or SPC:s characteristics noise therefore the results may not reflect how the QA would answer to visual wavelength cameras.

## 4 Evaluation

This section is structured as, for each experiment and setup a detailed explanation and motivation on how and why the experiment is needed followed by the results of that experiment. The experiments are motivated by gathering as much information and results as possible to answer the research questions. The first subsection 4.1 will present the results from experiments with synthetic data where a reference image is available. The second subsection 4.2 will present the result from images reconstructed from the SPC. No perfect reference image is available in those experiments therefore the images will be evaluated against near optimal image, no reference QA and against a state of the art SWIR camera.

### 4.1 Synthetic data

#### 4.1.1 PSNR, SNR, SSIM

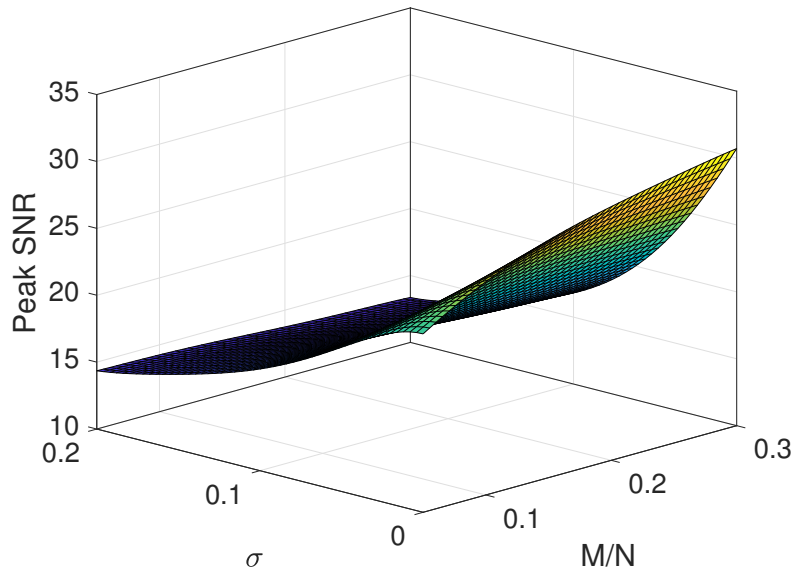


Figure 7: Peak SNR result depending on number of measurements and simulated noise level.

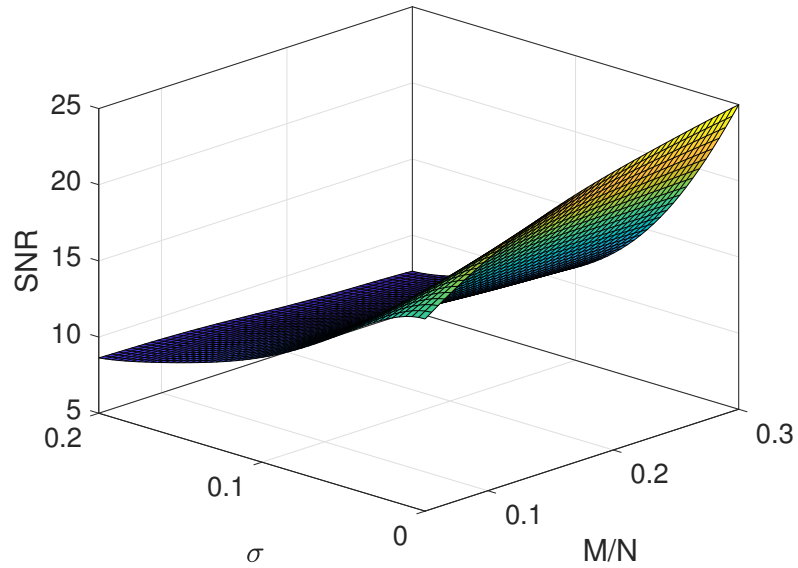


Figure 8: SNR result depending on number of measurements and simulated noise level.

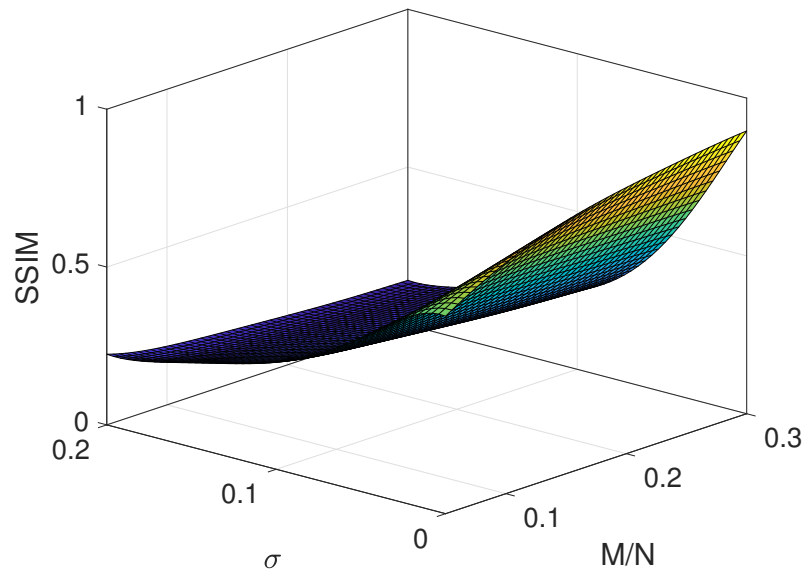


Figure 9: SSIM result depending on number of measurements and simulated noise level.

#### 4.1.2 No Reference quality assessment

BRISQUE lower score is better.

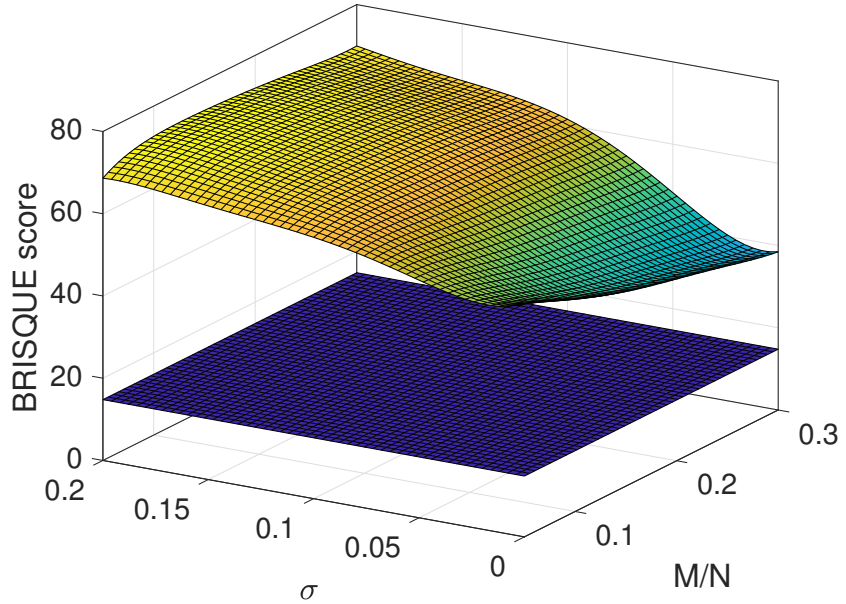


Figure 10: BRISQUE result depending on number of measurements and simulated noise level. Lower surface is reference image score.

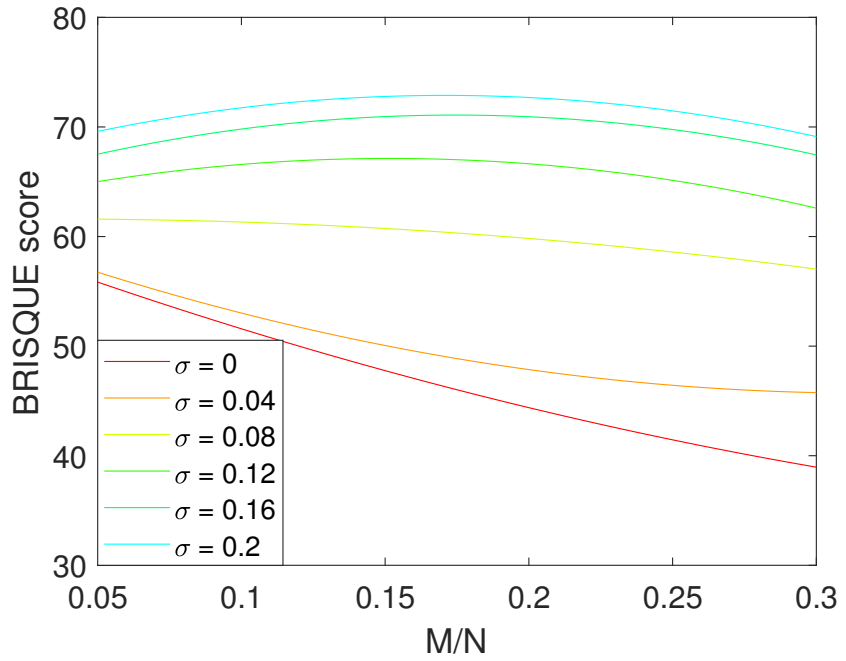


Figure 11: BRISQUE result depending on number of measurements for different simulated noise levels.

#### 4.1.3 Dynamics in scene

Dynamics in the scene can roughly be divided into three separate scenarios, in this section each of them will be tested in a controlled environment with each scenario isolated to show how the signal and the reconstructed image is effected.

In the first scenario a object will be placed in an image but for each measurement matrix the location of the object will be moved in a bounded area of the image. This will model as a scene where the background is static but a person is standing in the same spot but moving around.

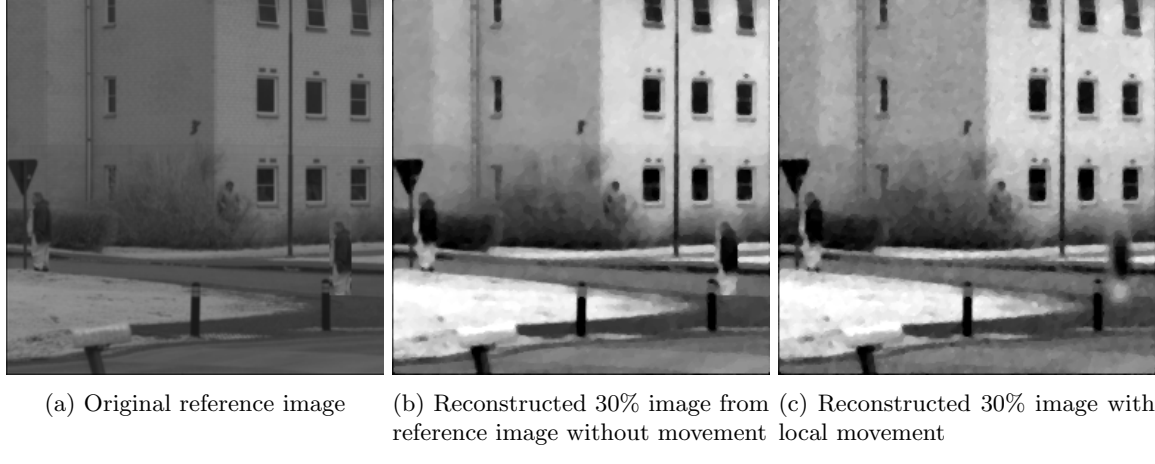


Figure 12: Local movement

The difference between figure 12b and 12c is visible with the naked eye, not only does the object moving around get blurry and noisy but the whole image globally. In table 2...

Peak SNR	SNR	SSIM
29	25	91

Table 2: Effects comparing non perturbed reconstructed image against reconstructed image with local movement

Commenting the result from the table... In figure 13 the effects of the movement is shown plotted against the non perturbed signal.

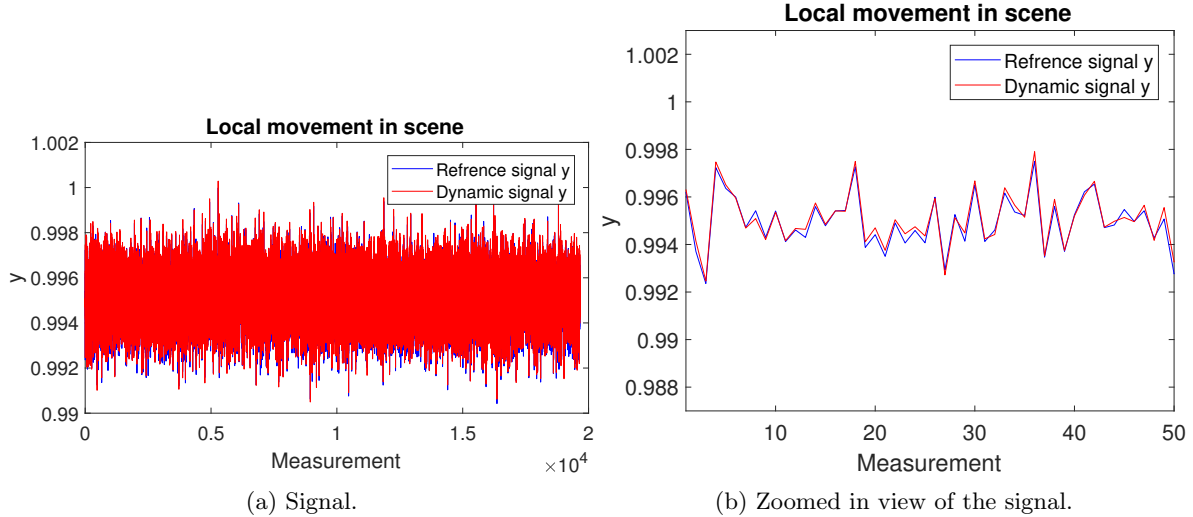


Figure 13: Local movement, acquired signal

As seen in figure 13a there is no obvious difference between the non perturbed reference signal and the distorted signal. In figure 12b where some of the samples is displayed no large difference can be seen ether, the conclusion of this test implies that local movement in a scene will cause noise in the image globally and especially locally where the movement occurred. It also implies that local movement is very hard to detect on the signal even if a reference signal is available.

The second scenario is an object is passing through, moves out or moves to an other place in the scene far from the original place. In other words, large global movement in the scene. The problem is modeled with a static background then as the simulated measurement is acquired the same object as in the first experiment will cross the scene, like a car, human or animal might do when using the SPC. The object will cross the scene in 1000 measurements of approximately 19000, corresponding to approximately 0.7 seconds when capturing with the SPC in its current setup.

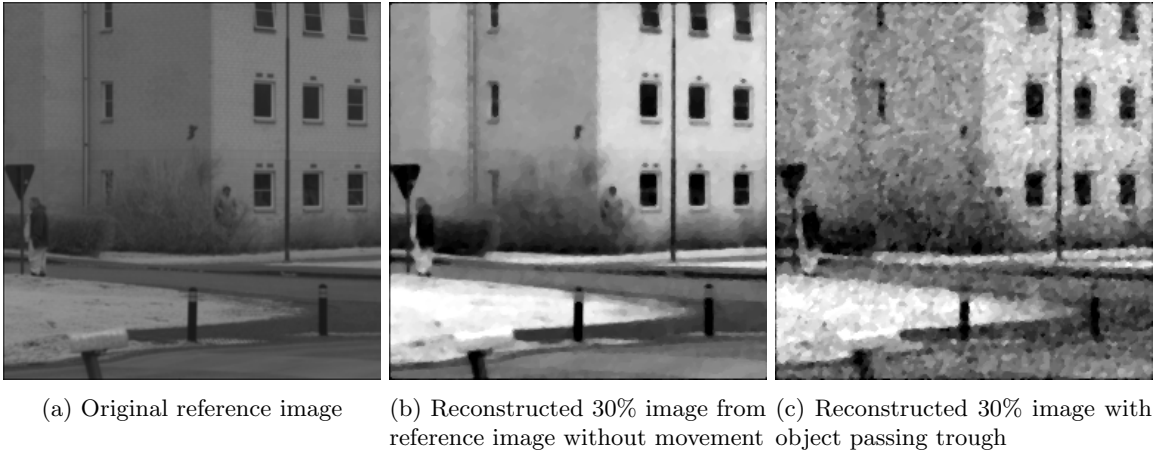


Figure 14: Object passing through scene.

The difference between figure 14b and 14c is visible with the naked eye, A global noise arises in the image and the object cant be seen. In table 3...

Peak SNR	SNR	SSIM
23	18	58

Table 3: Effects comparing non perturbed reconstructed image against reconstructed image with local movement

Commenting the result from the table... In figure 15 the effects of the movement is shown plotted against the non perturbed signal.

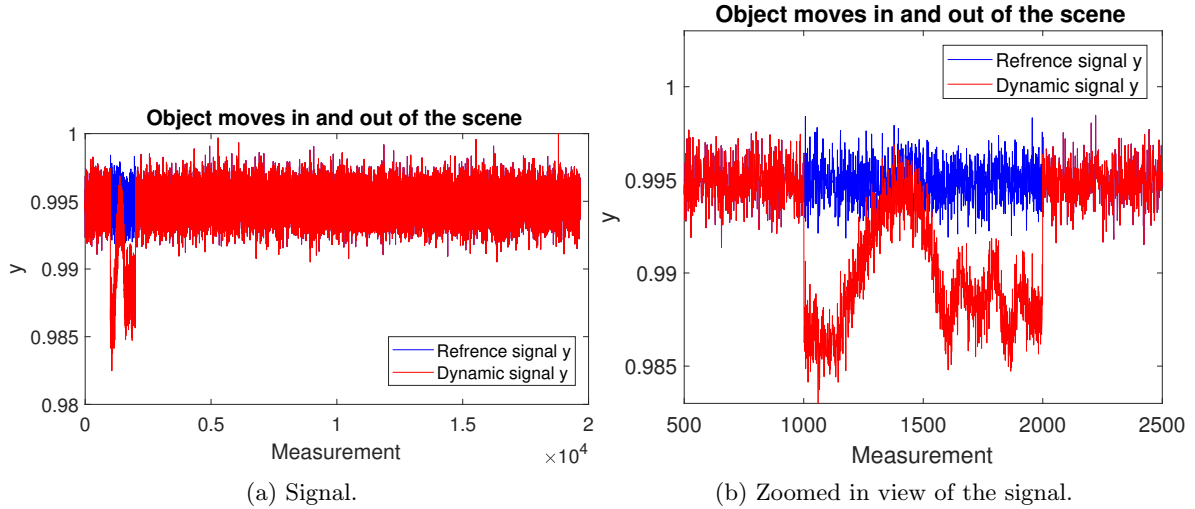


Figure 15: Global movement, acquired signal

- Large changes in the scene can be detected
- Remove the identified measurements to get a good signal

The third scenario i luminance change in the scene caused by clouds occludes the sun or the light intensity from the lights is not constant. This scenario is modeled by adding or subtracting the global intensity in the image over the measurements.

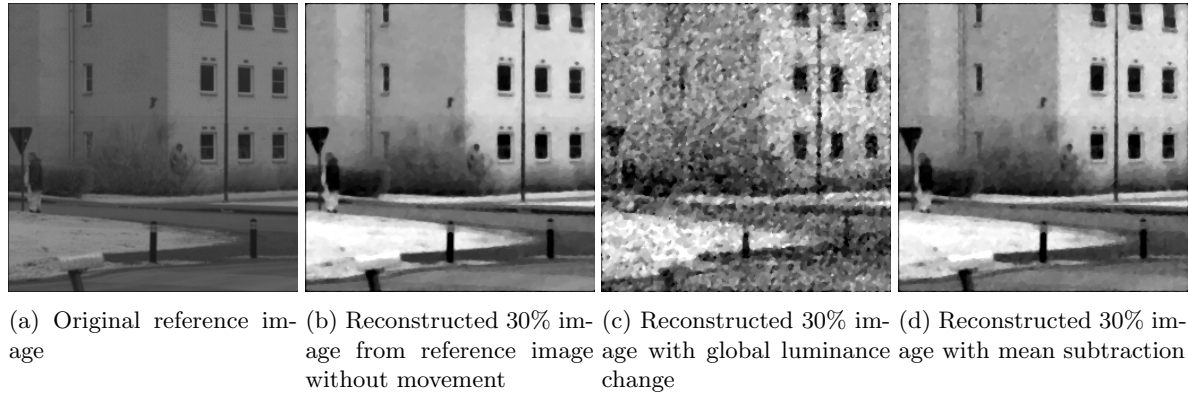


Figure 16: Global luminance change in scene.

The difference between figure 16b and 16c is visible with the naked eye, A global noise arises in the image, but as seen in figure 16d the effect can be suppressed explained under figure 17. In table 3...

	Peak SNR	SNR	SSIM
Perturbed signal	19	14	38
Mean subtracted signal	33	29	93

Table 4: Effects comparing non perturbed reconstructed image against reconstructed image with global luminance change

Commenting the result from the table... In figure 17 the effects of global luminance is shown plotted against the non perturbed signal.

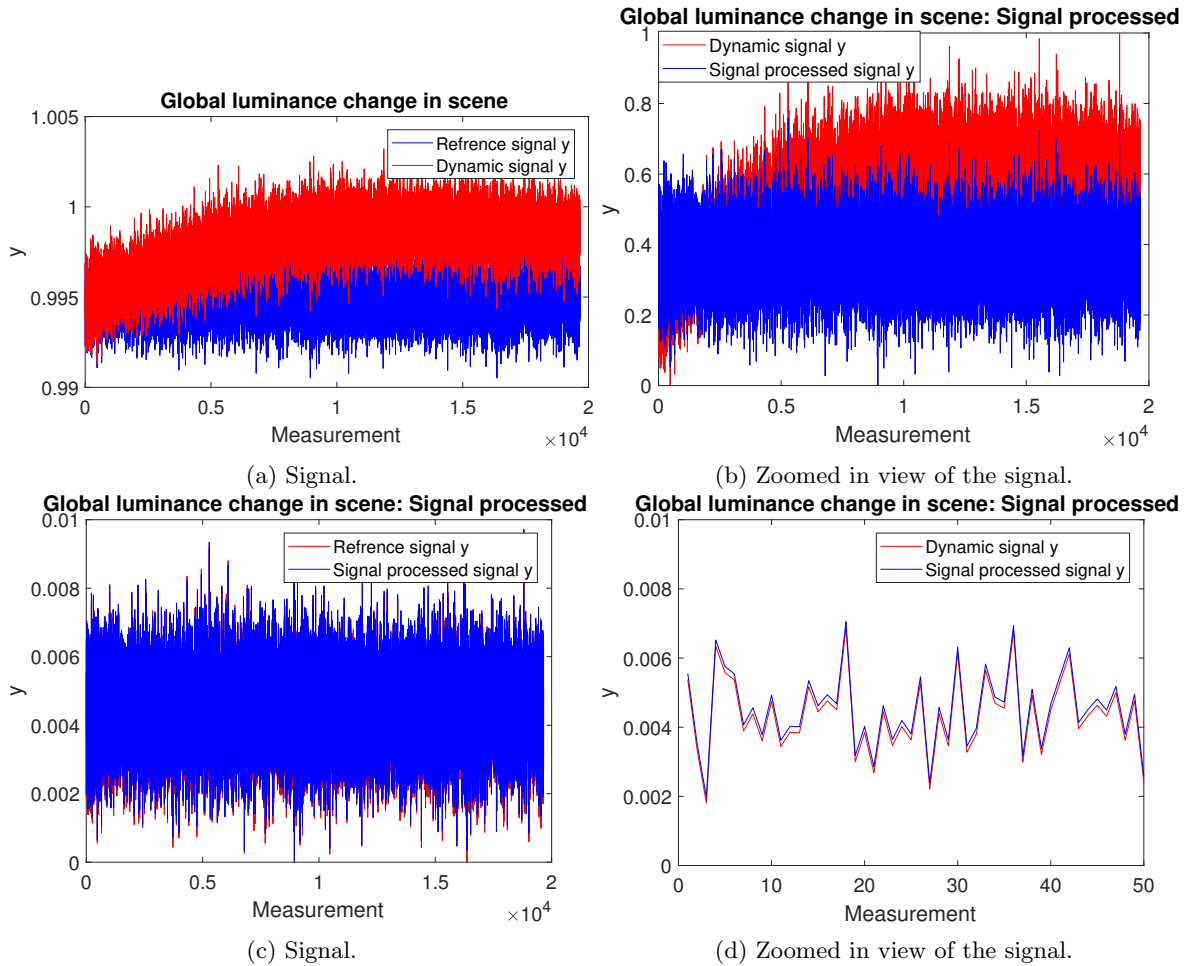


Figure 17: Global movement, acquired signal

- Dynamic signal v. Reference signal
- Dynamic signal v. Mean subtracted signal
- Reference signal v. Mean subtracted signal
- Comment on the window, pretty good.
- Can be detected with the knowledge that the signal should be stationary. Signal process the signal to look like a stationary signal.

## 4.2 SPC evaluation

### 4.2.1 Number of measurements

#### 4.2.2 Soft chessboard

Todo: Skapa rekonstruerade bilder från homographin och jämför de rekonstruerade med referensbilden

This evaluation is designed to confirm that the images reconstructed by the SPC follows the same characteristics as the reconstruction of the synthetic data.

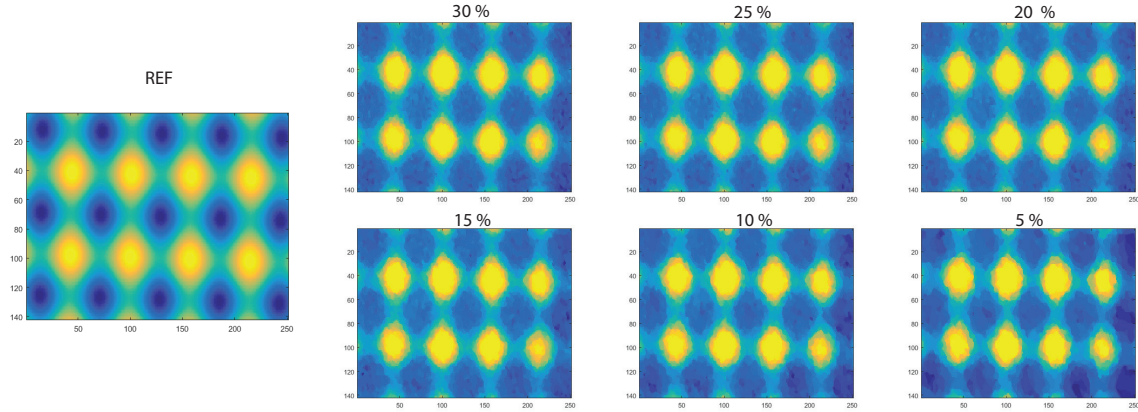
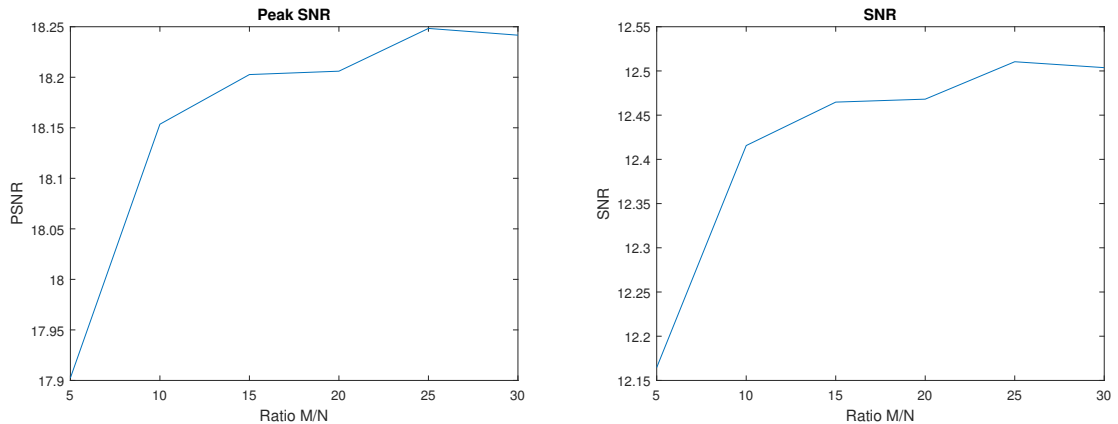
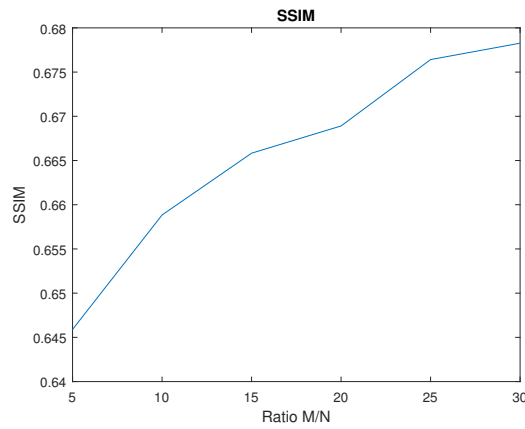


Figure 18: The reconstructed images with different number of measurements and the reference image transformed to fit the SPC images using homography.



(a) Peak SNR for reconstructed images against reference image. (b) SNR for reconstructed images against reference image.



(c) SSIM score for reconstructed images against reference image.

Figure 19: Signal quality of SPC images compared to reference image

#### 4.2.3 No reference quality assessment

Using the no reference quality assessment measurement BRISQUE to evaluate the SPC images. Each image is evaluated at reconstruction rate 5% to 30%.

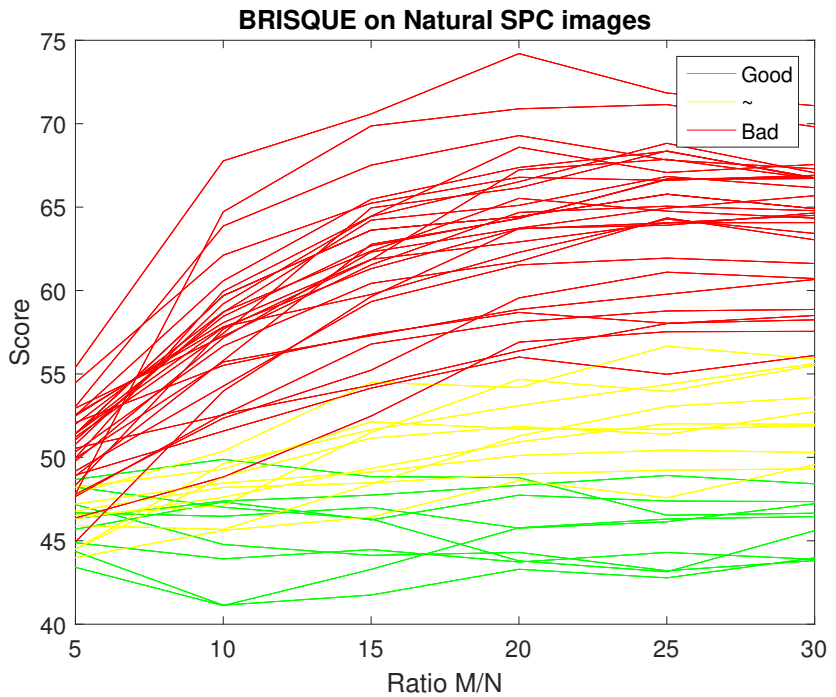


Figure 20: BRISQUE result.



Figure 21: Example of 'good' images corresponding to the green lines in figure 20.



Figure 22: Example of 'medium good' images corresponding to the yellow lines in figure 20.

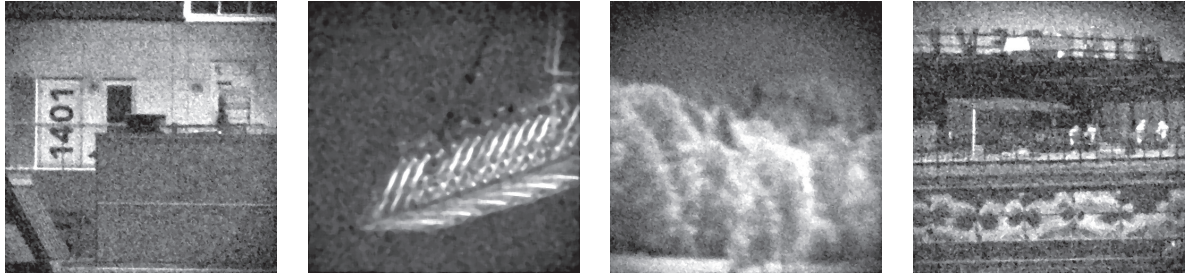


Figure 23: Example of 'bad' images corresponding to the red lines in figure 20.

- Good images are:
- Medium good images are:
- Bad images are:

#### 4.2.4 Modulation Transfer Function

The MTF is used to comparing the sharpness of cameras and lenses.

The MTF from the SPC is compared to a state of the art SWIR camera. Two scenes was captured by the SPC and a conventional SWIR camera containing printed sheath of paper with simple tilted shapes on them, see figure 24.

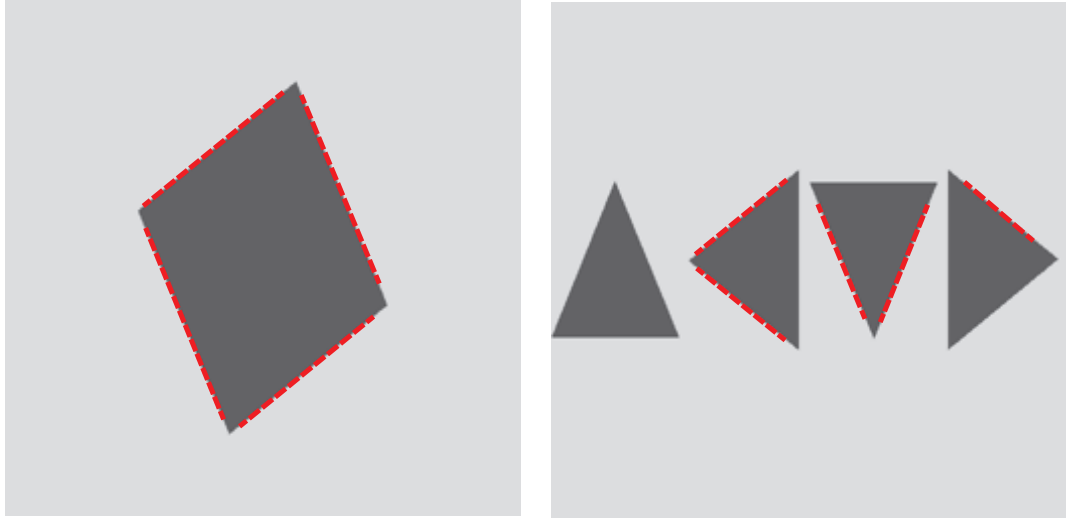


Figure 24: Printed targets with markings where the MTF measurements was performed

In the resulting images MTF measurements was performed on the specified edges to gather a mean and standard deviation for each camera. For the SPC, images reconstructed from 5% to 30% was tested in order to see if the number of measurements effected the MTF result. In figure 25 the images from the SWIR camera and SPC are presented.

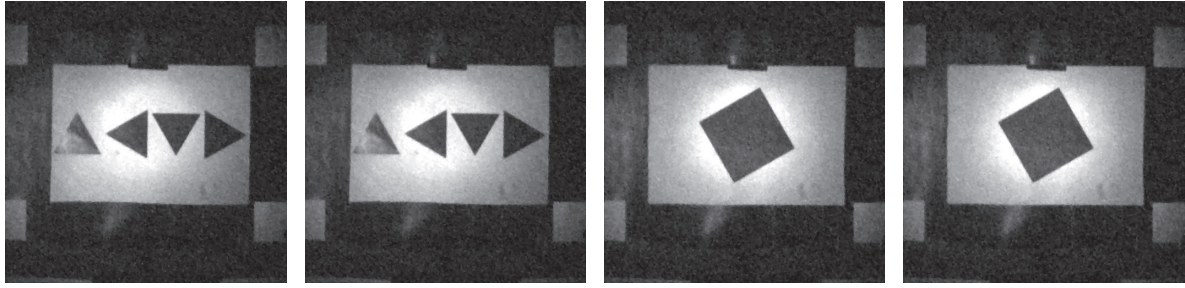


Figure 25: SPC and state of the art SWIR camera output images. (OBS! Bilder från Raptorn ska läggas till)

### 4.3 MTF

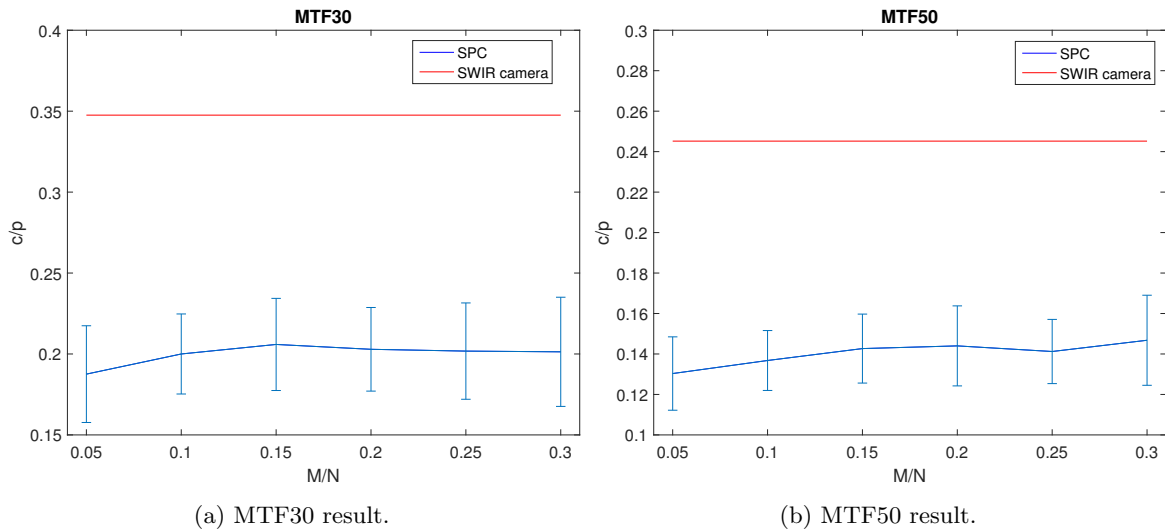


Figure 26: MTF results. (OBS! inte rätt figurer)

### 4.4 Edge response

The edge response is measured in the distance (pixels) required for the edge to rise from 10% to 90%. In figure 27 the result from the experiment is presented.

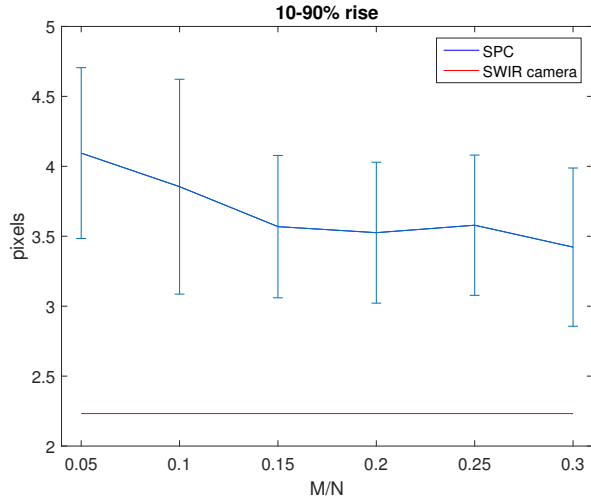


Figure 27: 10-90% rise in pixels. (OBS! inte rätt figur)

## References

- [1] D. L. Donoho, “Compressed sensing,” *IEEE Transactions on Information Theory*, vol. 52, no. 4, pp. 1289–1306, Apr. 2006, ISSN: 0018-9448. DOI: 10.1109/TIT.2006.871582.
- [2] T. T. Do, L. Gan, N. H. Nguyen, and T. D. Tran, “Fast and efficient compressive sensing using structurally random matrices,” *IEEE Transactions on Signal Processing*, vol. 60, no. 1, pp. 139–154, Jan. 2012, ISSN: 1053-587X. DOI: 10.1109/TSP.2011.2170977.
- [3] A. Bovik, *The Essential Guide to Image Processing*. Elsevier, 2009, ISBN: 978-0-12-374457-9.
- [4] L. Zhang, L. Zhang, and A. C. Bovik, “A feature-enriched completely blind image quality evaluator,” *IEEE Transactions on Image Processing*, vol. 24, no. 8, pp. 2579–2591, Aug. 2015, ISSN: 1057-7149. DOI: 10.1109/TIP.2015.2426416.
- [5] C. Brännlund and D. Gustafsson, “Single pixel swir imaging using compressed sensing,” *Symposium on Image Analysis, 14-15 March 2017, Linköping, Sweden*, 2017.
- [6] L. Duval, *50mm f1 swir fixed focal length lens*, Edmund Optics Inc, 2017. [Online]. Available: <https://www.edmundoptics.com/imaging-lenses/fixed-focal-length-lenses/50mm-f1-swir-fixed-focal-length-lens/> (visited on 05/17/2017).
- [7] *Large area ingaas amplified photodetectors pda20c operation manual*, 1.1, Thorlabs GmbH, Sep. 2016. [Online]. Available: [https://www.thorlabs.com/drawings/e22761fd83df1eab-B1D1D2AA-C921-6D8E-D2B14E11544D8225/PDA20C\\_M-Manual.pdf](https://www.thorlabs.com/drawings/e22761fd83df1eab-B1D1D2AA-C921-6D8E-D2B14E11544D8225/PDA20C_M-Manual.pdf) (visited on 05/16/2017).
- [8] “Maximum length sequence encoded hadamard measurement paradigm for compressed sensing.,” *2014 IEEE/ASME International Conference on Advanced Intelligent Mechatronics, Advanced Intelligent Mechatronics (AIM) Besancon, France, July 8-11, 2014*, pp. 1151–1156, 2014, ISSN: 978-1-4799-5736-1.
- [9] C. Li, “An efficient algorithm for total variation regularization with applications to the single pixel camera and compressive sensing.,” 2009.